ACS OMEGA

Open Access

http://pubs.acs.org/journal/acsodf

Article

Paracetamol-Mediated Synthesis of Silver Nanoparticles and Their Functionalization with Ionic Liquid for the Colorimetric Biosensing of Ascorbic Acid

Umar Nishan,* Irfan Ullah, Rukhsana Gul, Amir Badshah, Nawshad Muhammad, Naeem Khan, Mohibullah Shah, Muhammad Asad, Saifullah Afridi, Riaz Ullah, Essam A. Ali, and Suvash Chandra Ojha*

Cite This: *ACS Omega* 2023, 8, 44931−44941

Read Online

ACCESS | Metrics & More | Article Recommendations

ABSTRACT: Ascorbic acid is a vital biomolecule for human beings. When the body's level of ascorbic acid is abnormal, it can lead to a number of illnesses. Its appropriate concentration is necessary for the oxidation of prostaglandins and cyclic adenosine monophosphate, the production of dopamine, norepinephrine, epinephrine, and carnitine, and the expansion and durability of the collagen triple helix in humans. In the present work, silver nanoparticle synthesis was performed through a paracetamol-mediated approach. Different characterization techniques, such as X-ray diffractometry (XRD), energy dispersive X-ray (EDX), Fourier transform infrared (FTIR), and scanning electron microscopy (SEM), were used to confirm the prepared nanoparticles. Subsequently, the prepared Ag NPs functionalized with an ionic liquid were used as a sensing platform for ascorbic acid in blood serum samples. To achieve the best possible results, the proposed biosensor was optimized with different parameters such as TMB concentration, time, amount of capped nanoparticles (NPs), and pH. The proposed biosensor offers a sensitive and straightforward method for ascorbic acid with a linear range from 2×10^{-9} to 3.22×10^{-7} M, an LOD of 1.3×10^{-8} M, an LOQ of 4.3×10^{-8} M, and an R^2 of 0.9996, Moreover, applications of the proposed biosensor were successfully used for the detection of ascorbic acid in samples of human plasma, suggesting that Ag NPs with high peroxidase-like activity, high stability, and facile synthesis exhibited promising applications in biomedical fields.

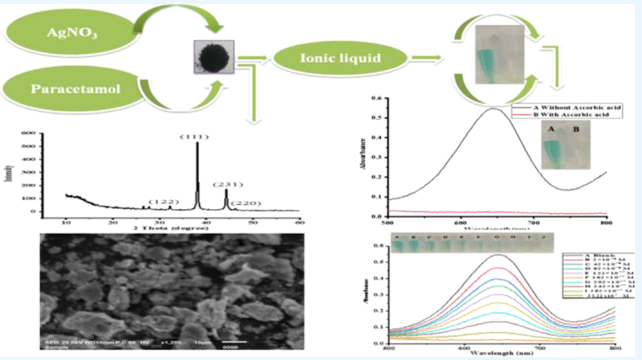

1. INTRODUCTION

The common water−soluble antioxidant ascorbic acid, generally known as vitamin C, is found in a variety of foods and beverages. In the food industry, it is added artificially to food sources as an antioxidant. Ascorbic acid is also essential for human survival.[1] Many human metabolism processes, such as cell differentiation, intestinal cells, iron uptake in humans, and immune functioning, depend on ascorbic acid.[2] Scurvy will arise from a deficiency of ascorbic acid, and urinary stones, diarrhea, and stomach convulsions are due to the abundance of ascorbic acid.[3,4] Rapid, sensitive, and selective detection of ascorbic acid levels is significant for medical testing and diagnosis.

For the determination of ascorbic acid, various methods have been reported, such as electrochemistry,[5] chromatography,[6] capillary electrophoresis,[7] and fluorescence spectroscopy.[8] Although these conventional approaches typically have good selectivity and a low detection limit, they frequently have some drawbacks, including costly, bulky equipment, and lengthy processes. The colorimetric approach has advantages including high sensitivity, quick analysis, and strong reproducibility due to its ease of use, speed, low cost, and ability to be easily detected with the naked eye. It has drawn a lot of attention and has attracted a lot of interest recently.

A wide range of applications, including environmental remediation, biosensors, biomedical devices, renewable energy, medicine, and cosmetics, have been developed due to the unique properties of nanoparticles. In comparison to their macroscale counterparts, due to their excellent chemical, biological, and physical properties, Ag nanoparticles (NPs) have attracted growing interest among these materials.[9]

Received: August 25, 2023
Revised: October 27, 2023
Accepted: November 7, 2023
Published: November 16, 2023

Nanomaterials have gained increasing interest over the past 10 years because of their distinctive, new characteristics and medicinal applications.[10] Due to their remarkable advantages, the use of colorimetric nanoprobes has significantly grown in recent years. Metal nanoparticles (NPs), primarily Au and Ag nanoparticles, exhibit extremely large molar extinction coefficients, sensitive colorimetric sensing due to their shape, distance-dependent optical characteristics, and unique size.[11]

Some new and effective fluorescent nanoprobes were developed based on their unique reaction between the nanomaterials and ascorbic acid. A potential method was developed for the determination of ascorbic acid.[12] For instance, Yan's et al. developed a CdTe QD fluorescence probe for the determination of ascorbic acid after quenching with a certain amount of $KMnO_4$.[1313] Similarly, cobalt oxyhydroxide (CoOOH)-modified persistent luminescence nanoparticles ($Sr_2MgSi_2O_7$:1% Eu, 2% Dy) designed in living cells and in vivo based on the specific reaction of CoOOH have been developed by Tang's et al. for the detection of ascorbic acid.[14] For in vivo sensing of ascorbic acid in rat brain, Mao's group developed a new fluorescent technique while examining the mechanism of single-layer MnO_2 nanosheets inhibiting luminous 7-hydroxycoumarin.[15] Gold or silver nanoparticles (Au or Ag NPs) are ideal chromogenic agents for the design of colorimetric sensors due to their distinctive size, structure,[16] and distance-dependent localized surface plasmon resonance (LSPR) properties.[17]

Agglomeration of nanoparticles is one of its features that has to be overcome, as it results in the loss of the available surface area for the reaction.[18] Ionic liquids that are conductive and have functional moieties in their structure can interact with the Ag NPs. They can interact through several intermolecular interactions, such as hydrogen bonding, steric, solvophobic, electrostatic, and van der Waals. All such types of interactions are proven to improve the sensing and catalytic properties of the sensing system.[19] 1-*H*-3-methylimidazolium acetate is a protic ionic liquid that has aromaticity in both the imidazolium cation and carboxylate anion. It helps in providing a more electron-rich conductive environment that eases reaction, while other nonaromatic protic ionic liquids do not have such resonance properties. Likewise, protic ionic liquids are preferred to aprotic ionic liquids, as the proton of such protic ionic liquids is suggested to play an important role in H_2O_2 degradation and subsequent detection.[20]

In this study, Ag NPs were prepared by using low-cost, docile, and ubiquitous paracetamol as a reductant. Moreover, the paracetamol-mediated Ag NPs were functionalized with 1-*H*-3-methylimidazolium acetate ionic liquid for excellent deagglomeration. The fabricated platform (paracetamol-mediated Ag NPs functionalized with IL) was used for the first time for colorimetric detection of ascorbic acid. By using H_2O_2, the chromogenic substrate, i.e., 3,3′,5,5′-tetramethylbenzidine (TMB), has been oxidized in the presence of IL/Ag NPs to develop a sensitive, selective, simple, and quick approach for the detection of the analyte. To achieve the best results of the proposed sensor, various reaction conditions, such as (a) pH, TMB concentration, time, and number of capped NPs, were optimized. The proposed biosensor sensitivity and selectivity were also investigated by using the aforesaid optimum conditions.

Scheme 1. Mechanism for the Determination of Ascorbic Acid

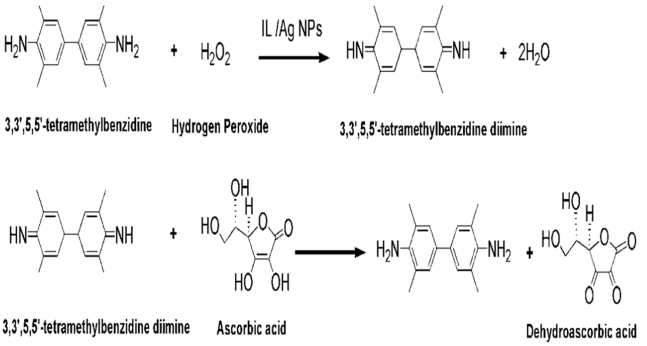

2. EXPERIMENTAL SECTION

2.1. Materials and Reagents. From Sigma-Aldrich, we purchased hydrochloric acid (HCl), 3,3′,5,5′-tetramethylbenzidine (TMB), silver nitrate ($AgNO_3$), hydrogen peroxide (H_2O_2), and sodium hydroxide (NaOH). BioWorld provided PBS at a range of pH levels. Paracetamol tablets (500 mg) were purchased from a local market. All of these substances were found in their purest forms and were used without further purification. The tests were conducted using premium glassware, and the solutions were prepared by using deionized water.

2.2. Instrumentation. To identify the characteristic peaks of Ag NPs, Fourier transform infrared spectroscopy (FTIR, Nicolet 6700) was used. Scanning electron microscopy (SEM), INCAx-act Oxford Instruments' TESCAN VEGA (LMU), was used to confirm the morphology of the prepared Ag NPs. The phase identification of the synthesized Ag NPs was carried out using X-ray diffraction (JCPDS, file No. 04-0783). The absorbance spectrum of the colloidal sample was obtained in the range of 200−800 nm with distilled water as a reference. Shimadzu's UV−vis spectrophotometer, model 1800, from Japan, was utilized to record the sample's absorption spectra.

2.3. Synthesis of Drug-Mediated Ag NPs. Two paracetamol tablets (500 mg) were ground into a fine powder and poured into 50 mL of double-distilled water to dissolve. At room temperature, the suspension was agitated for 10 min at a speed of 1000 rpm, and after stirring, the solution was filtered. A 50 mM solution of $AgNO_3$ was prepared and added dropwise to the obtained filtrate while being kept at 1000 rpm on a magnetic stirrer for 6 h at an ambient temperature. The solution changed from colorless to brown as it was mixed. In order to obtain Ag NPs in powder form, the solution containing Ag NPs was stirred and centrifuged for 25 min. The Ag NPs were maintained at room temperature after being dried at 50 °C for further use in characterization and sensing.

2.4. Characterization. For the confirmation of prepared nanoparticles, different characterization techniques were used such as scanning electron microscopy (SEM), X-ray diffraction (XRD), UV−vis spectroscopy, energy-dispersive X-ray analysis (EDX), and Fourier transform infrared spectroscopy (FTIR).

2.5. Synthesis of Ionic Liquid. 1-*H*-3-methylimidazolium acetate ionic liquid was synthesized using the modified approach that was previously published by our group.[21−23]

2.6. Capping of Drug-Mediated Ag NPs with Ionic Liquid. The prepared 1-*H*-3-methylimidazolium acetate ionic liquid (IL) was capped with synthesized Ag NPs. One mL of the ionic liquid was mixed with Ag NPs (6 mg). The mixture

https://doi.org/10.1021/acsomega.3c06353
ACS Omega 2023, 8, 44931−44941

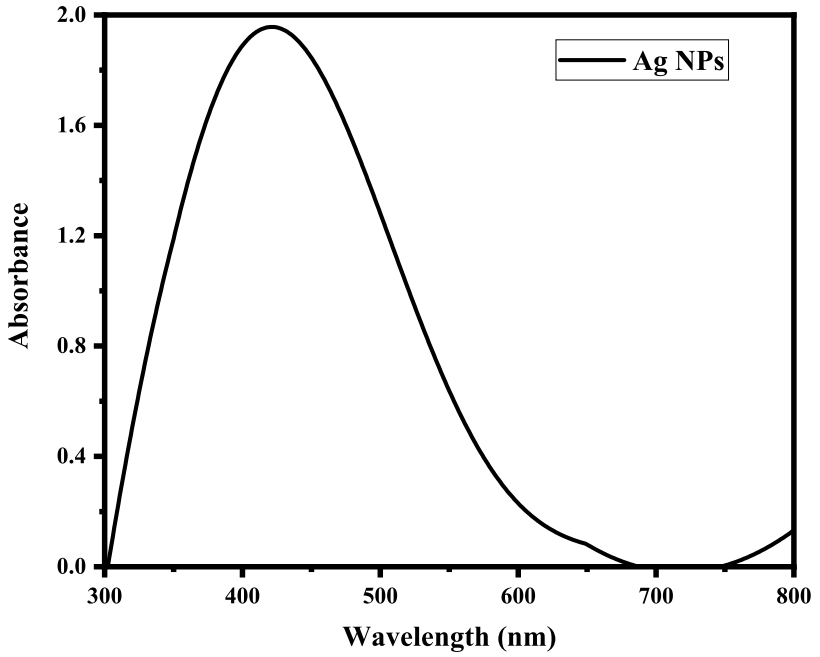

Figure 1. UV−vis absorption spectrum of the paracetamol-mediated Ag NPs showing the characteristic surface plasmon resonance and peak at around 417 nm.

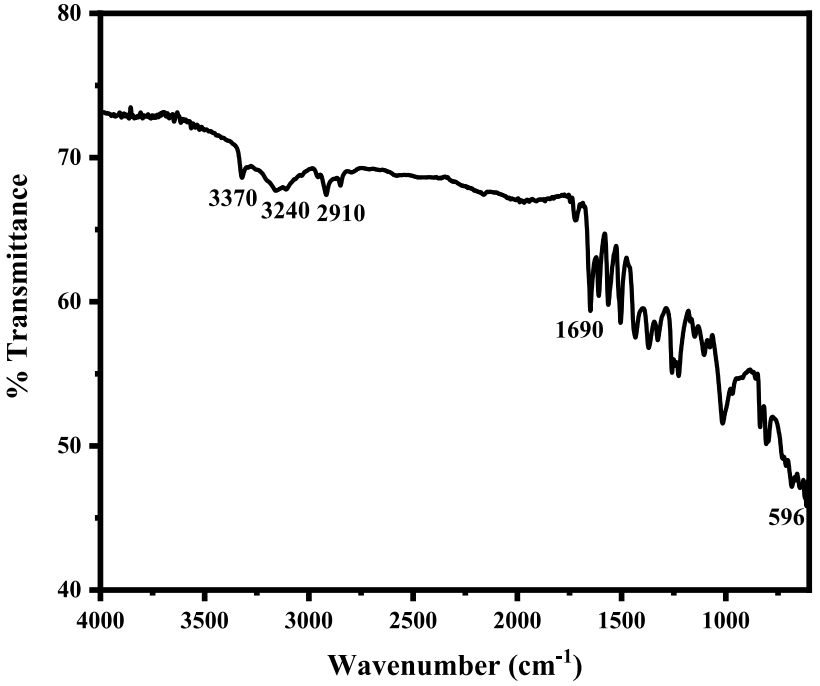

Figure 2. FTIR spectrum of the drug-mediated Ag NPs shows the presence of Ag−O, confirming the formation of Ag NPs in the presence of a capping agent.

was thoroughly crushed for 30 min using a pestle and mortar. The functionalized Ag NPs were stored for further analysis.

2.7. Colorimetric Detection of Ascorbic Acid. Ag NPs were evaluated for their peroxidase-like activity by using colorimetric detection. The 3,3′,5,5′-tetramethylbenzidine (TMB) dye was expected to be oxidized by H_2O_2, and the product's color will change from colorless to blue-green. The reaction occurred under the following conditions: 40 μL of IL/Ag NPs 4 mM TMB solution (180 μL) and 500 μL of acetate buffer solution, followed by the addition of 9 mM H_2O_2 solution (200 μL). Then, 90 μL of ascorbic acid (3.22×10^{-7} M) was added to the reaction solution, and the mixture was then incubated. Both the UV−vis spectrophotometer and the naked eye confirmed the expected colorimetric change (Scheme 1).

3. RESULTS AND DISCUSSION

3.1. Characterization of Silver Nanostructures. *3.1.1. UV−Visible Absorption Studies.* The synthesis of Ag NPs was investigated using UV−vis spectrum analysis. The

https://doi.org/10.1021/acsomega.3c06353
ACS Omega 2023, 8, 44931−44941

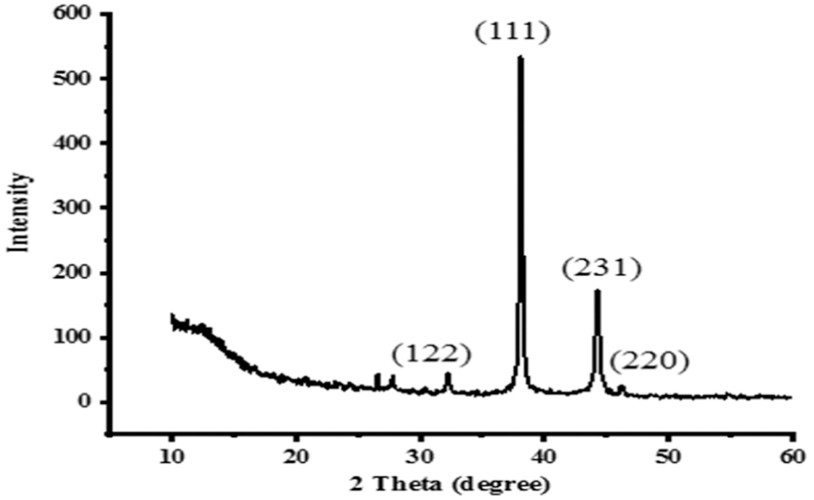

Figure 3. XRD analysis of the prepared face-centered cubic Ag NPs with an average crystalline size of 42 nm.

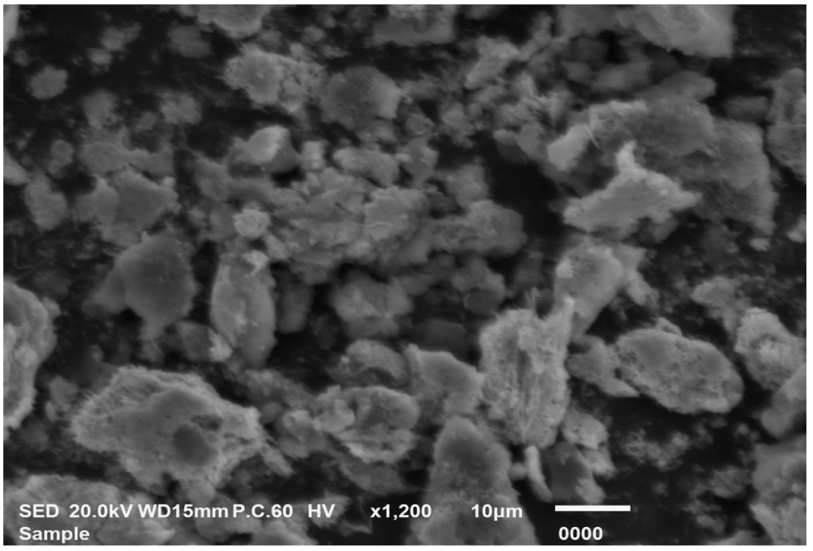

Figure 4. SEM image of the synthesized Ag NPs shows that the prepared nanoparticles have a strong agglomeration tendency.

color change was observed with the combination of paracetamol tablets and silver nitrate solution. During the reduction process, visual observation of the reaction solution's color changing from colorless to brown confirms the synthesis of drug-mediated Ag NPs. For 1 week, the absorbance of the solution was investigated. According to the spectrum analysis, the Ag NP peak was observed at 417 nm, as shown in Figure 1, and it remained stable for a few days. After that, no absorption increase was observed.[24]

3.1.2. FTIR Analysis. The FTIR spectra of the synthesized nanoparticles are shown in Figure 2. FTIR characterization of the drug-mediated nanoparticles was carried out in the region of 4000−500 cm^{-1}. The characteristic peak at around 2910 cm^{-1} was assigned to CH_3 in the acetyl group of the paracetamol. The absorption bands at around 3240 and 3370 cm^{-1} are assigned to the NH and OH bonds of the drug-mediated Ag NPs. The peak at around 1690 cm^{-1} was allocated to C═O, and the band at 596 cm^{-1} was assigned to the presence of Ag−O, confirming the formation of Ag NPs in the presence of a capping agent.[25,26]

3.1.3. XRD Analysis. Various Bragg reflections of the synthesized Ag NPs were confirmed by XRD analysis, which can be found at 2θ (°) values of 33.1, 38.12, 44.3, and 46.39°, which relate to the planes of pure Ag 111, 122, 220, 231, and 241 dependent on the face-centered cubic structure (JCPDS, file No. 04-0783), as illustrated in Figure 3. The synthesized Ag NPs were crystalline in nature, which was confirmed by X-ray diffraction.[27] The prepared face-centered cubic Ag NPs' average crystal size was calculated to be 42 nm. The average crystalline size of the prepared Ag NPs was calculated by using the Scherrer equation ($D = K\lambda/\beta \cos\theta$).

3.1.4. SEM Analysis. To examine the morphology of silver nanoparticles, scanning electron microscopy (SEM) was used, as shown in Figure 4. The prepared nanoparticles have a strong tendency toward agglomeration, have round-shaped structures, and are crystalline in nature. The SEM pictures reveal that the produced nanoparticles feature granular aggregates, cluster structures, and a high tendency toward agglomeration. In addition to the particles, there was a material that might be connected to the precursors.[28,29]

3.1.5. EDX Analysis. Figure 5 and Table 1 show the presence of Ag particles as well as the primary components of C and O, which come from the drug coating. For the synthesis of nanoparticles, $AgNO_3$ salt was used. Certain impurities of Si

https://doi.org/10.1021/acsomega.3c06353
ACS Omega 2023, 8, 44931−44941

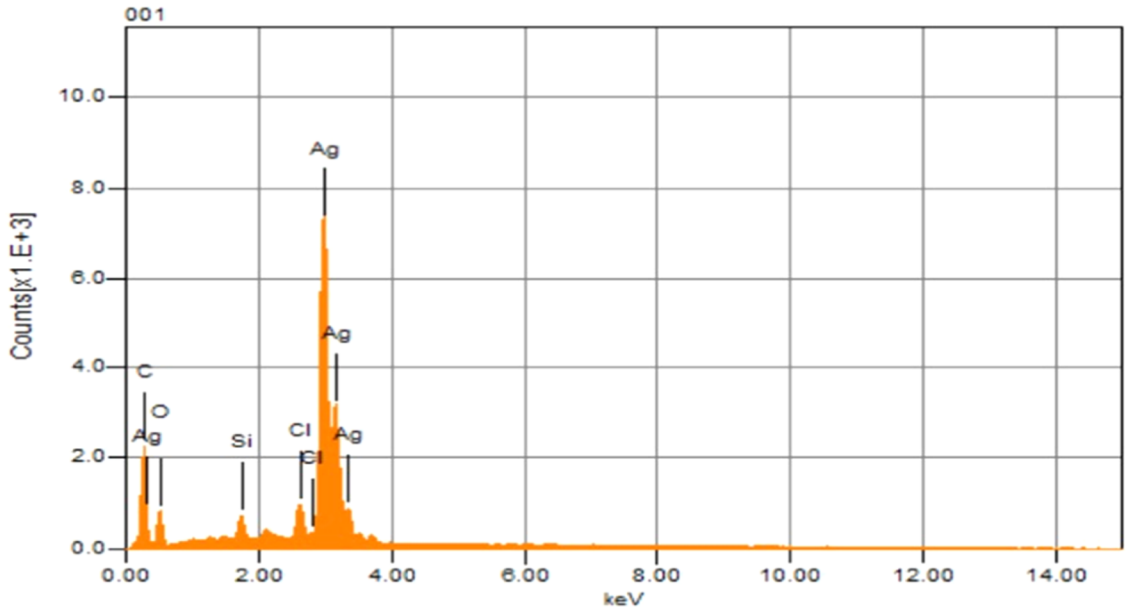

Figure 5. EDX spectrum of the synthesized Ag NPs shows a strong Ag peak.

Table 1. EDX Analysis by Weight of the Synthesized Ag NPs

element	weight %	atomic %
C	12.09	36.78
O	15.88	36.28
Si	1.47	1.91
Cl	1.61	1.66
Ag	68.96	23.37
total	100.00	100.00

and Cl were also found that may be due to the SEM sample tape and chemicals.

3.2. Colorimetric Detection of Ascorbic Acid. For the detection of ascorbic acid, a simple and selective colorimetric approach based on Ag NPs was developed. Figure 6 illustrates the optical sensing and UV−vis absorption spectra of ascorbic acid. Ascorbic acid decreases the blue−green byproducts when it is added to oxidize TMB. Additionally, the formation of OH radicals from the adsorption of hydrogen peroxide on the surface of NPs is linked to the oxidation of TMB to generate blue−green compounds. When ascorbic acid was added to the reaction mixture, the blue−green product was further decreased to colorless within 2 min. The solution was initially blue−green, but after the addition of ascorbic acid, it turned colorless, which can be observed with the naked eye. The colorimetric change can also be observed by the UV−vis spectrum, as can be seen in Figure 6. Previously, Liu et al. used Pt/CeO_2 nanocomposites for the colorimetric detection of ascorbic acid.[30]

3.3. Mechanism for the Detection of Ascorbic Acid. In the proposed mechanism, TMB is oxidized by hydrogen peroxide mediated by IL-functionalized Ag NPs. This results in the formation of a blue-green product, which confirms the

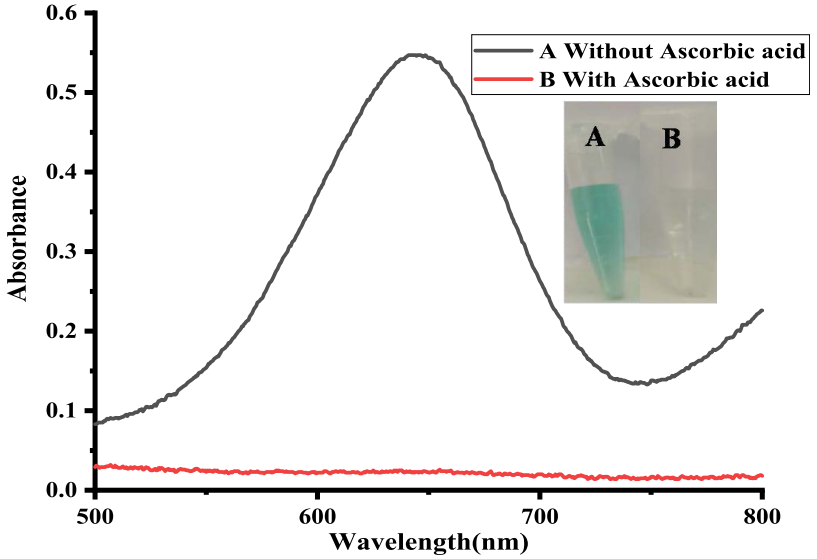

Figure 6. Colorimetric detection of ascorbic acid conditions: 40 μL of capped Ag NPs, μL of TMB sol (4 mM), 500 μL of PBS (0.2 mM), 200 μL of H_2O_2 (9 mM), and 90 μL of ascorbic acid (3.22×10^{-7} M).

https://doi.org/10.1021/acsomega.3c06353
ACS Omega 2023, 8, 44931−44941

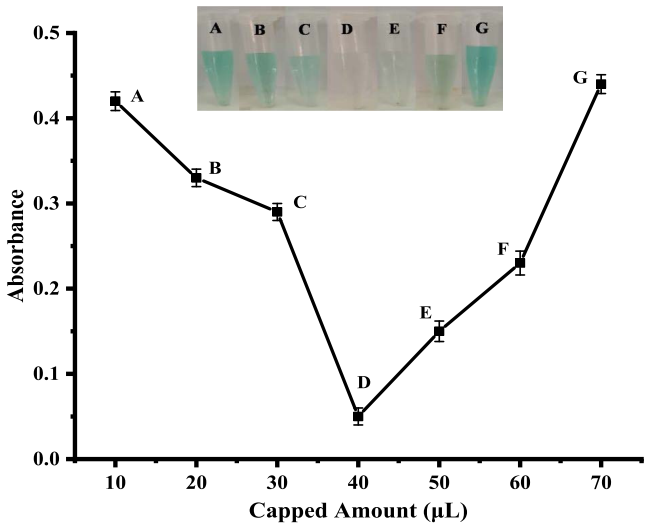

Figure 7. Effect of capped Ag NPs [conditions: 180 μL of TMB sol (4 mM), 500 μL of PBS (6 mM), 70 μL of H_2O_2 (9 mM), and 90 μL of ascorbic acid (3.22×10^{-7} M)].

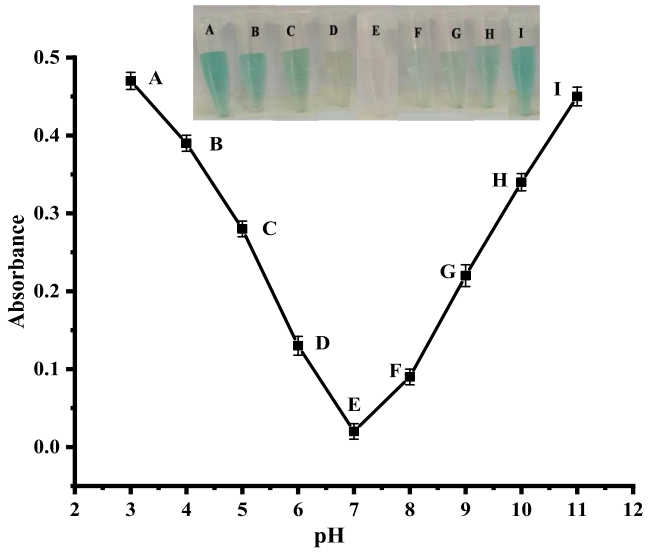

Figure 8. pH optimization of the proposed biosensor [conditions: 40 μL of capped Ag NPs, 180 μL of TMB sol (4 mM), 200 μL of H_2O_2 (9 mM), and 90 μL of ascorbic acid (3.22×10^{-7} M)].

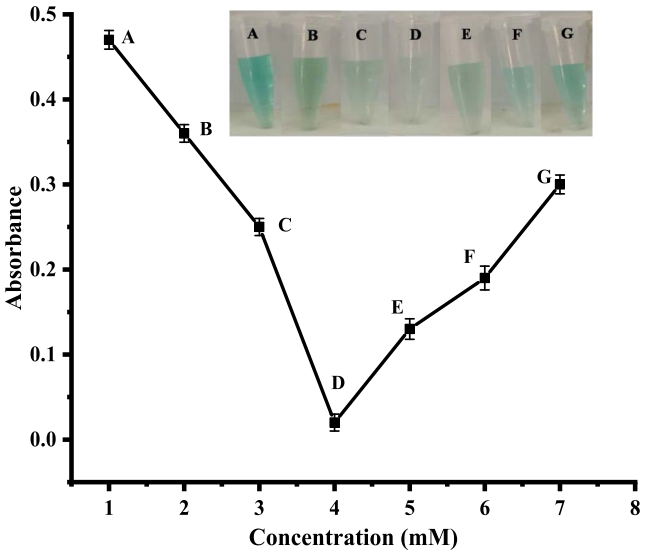

Figure 9. Optimization of the TMB solution [conditions: 40 μL of capped Ag NPs, 500 μL of PBS (6 mM), 200 μL of H_2O_2 (9 mM), and 90 μL of ascorbic acid (3.22×10^{-7} M)].

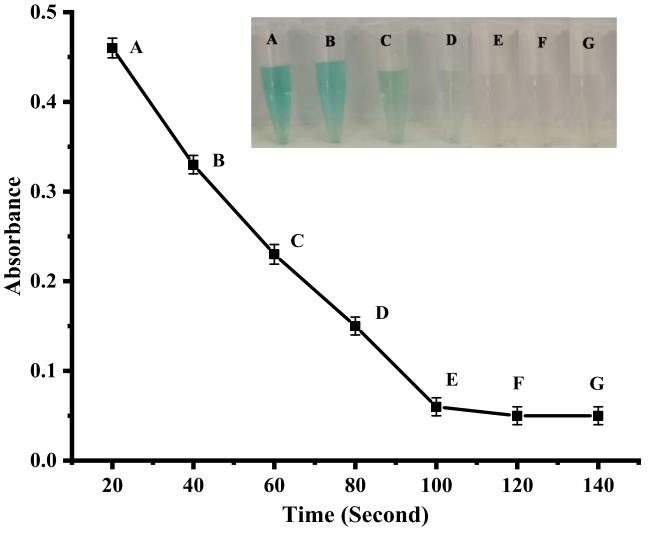

Figure 10. Time optimization [conditions: 40 μL of capped Ag NPs, 180 μL of TMB sol (4 mM), 500 μL of PBS (6 mM), 200 μL of H_2O_2 (9 mM), and 90 μL of ascorbic acid (3.22×10^{-7} M)].

oxidation of TMB. The addition of ascorbic acid to the reaction mixture results in the reduction of oxidized TMB (colorless), where the ascorbic acid acts as a reducing agent and converts to dehydroascorbic acid. Chen et al. also reported a peroxidase mimic platform of Pt-loaded hollow mesoporous carbon nanospheres for the colorimetric detection of ascorbic acid.[31]

3.4. Optimization of Different Parameters. *3.4.1. Optimization of Capped Ag NPs.* The optimization of the capped Ag NPs was performed, and the results are shown in Figure 7. In an Eppendorf tube, different amounts of IL-coated NPs were added: 200 μL of H_2O_2, 500 μL of phosphate-buffer saline solution, 4 mM of TMB solution (180 μL), and 90 μL of an ascorbic acid solution with a concentration of 3.22×10^{-7} M. To observe the colorimetric shift, the reaction was allowed to run for 2 min. 90 μL of ascorbic acid and 40 μL of ionic liquid-capped silver nanoparticles are synergistic. In other words, the color entirely shifts from green to translucent at a 40 μL capped Ag NP quantity. So, 40 μL of capped Ag NPs were selected as the optimum concentration for further analysis.[32−34]

3.4.2. pH Optimization. Figure 8 shows the optimal pH for the suggested reaction. To efficiently manage the suggested sensor's response, different pH values within the range of 3−11 were used. NaOH and HCl solutions were originally used in order to optimize the pH properly. The following optimal circumstances led to the best colorimetric shift for the suggested sensor: 40 μL of IL/Ag NPs, 200 μL of H_2O_2, incubation time 2 min, 180 μL of TMB solution (4 mM), and 90 μL of ascorbic acid solution (3.22×10^{-7} M). Therefore, for further experiments, pH 7 was selected as the optimum pH. Therefore, pH 7 that was measured is the optimal pH for the recommended probe. In the previously reported work, 6.59

https://doi.org/10.1021/acsomega.3c06353
ACS Omega 2023, 8, 44931−44941

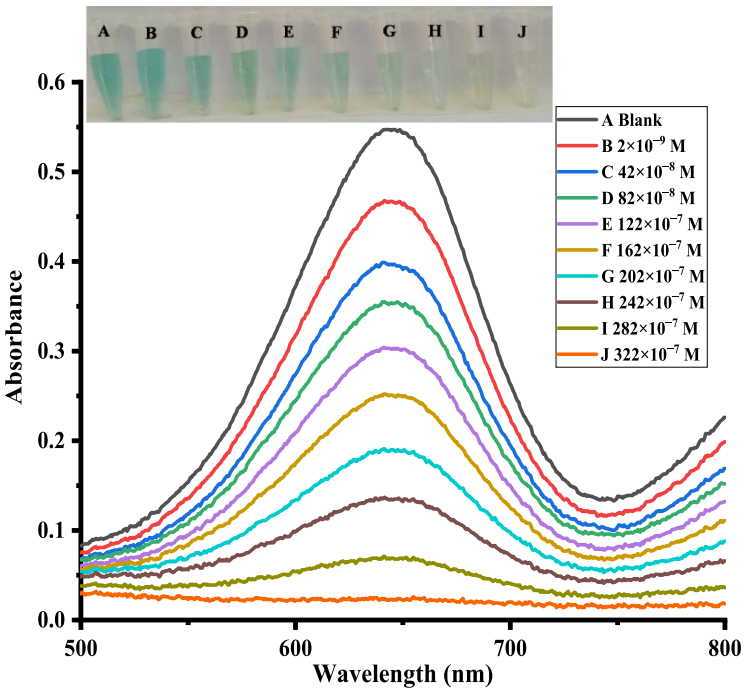

(A)

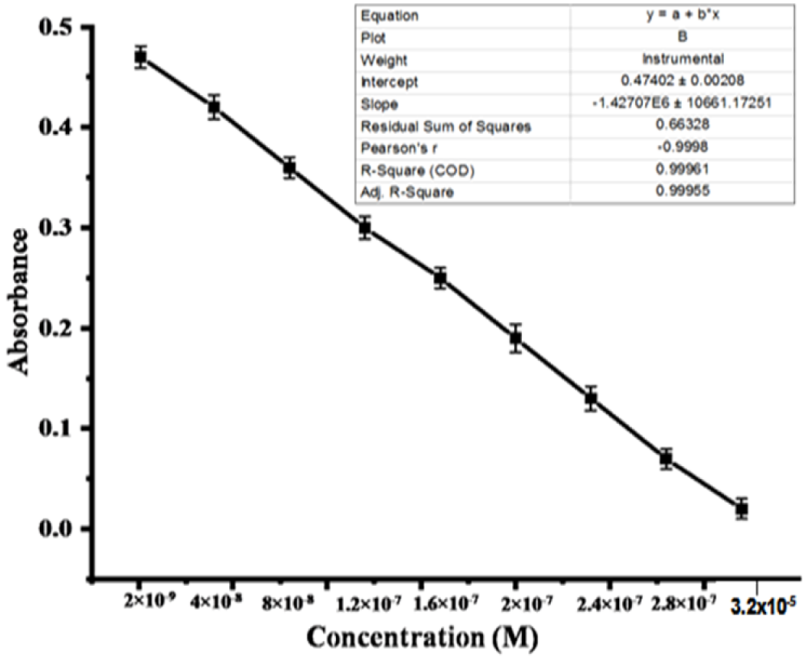

(B)

Figure 11. Panel (A) shows different concentrations of ascorbic acid, and panel (B) shows the corresponding calibration curve.

was suggested as the ideal pH for the recommended biosensor.[35]

3.4.3. TMB Optimization. To accomplish the best colorimetric change, the TMB concentration was also optimized. TMB solutions at a range of concentrations, from 1 to 7 mM, were prepared. When ascorbic acid was added, the reaction mixture became colorless, and the sensor gave the best response with a 4 mM TMB solution. Figure 9 shows that the colorimetric response did not perform well at lower or higher concentrations of TMB than 4 mM. So, the optimum concentration of TMB for further experiments was determined to be 4 mM.[36]

3.4.4. Time Optimization. Time intervals ranging from 20 to 140 s were observed on the sensors. After 120 s of incubation, excellent colorimetric changes were detected, as shown in Figure 10. At that point, all of the capped Ag NPs were used in the reaction. As a result, for further experiments, 120 s was selected as the optimum time because no further colorimetric change was observed after 120 s.

https://doi.org/10.1021/acsomega.3c06353
ACS Omega 2023, 8, 44931−44941

Table 2. Comparison of Some of the Colorimetric Sensors with the Proposed Biosensor for Detection of Ascorbic Acid

S. no	materials used	method applied	linear range (μM)	LOD (μM)	references
1	Pt/CeO_2 nanocomposites	colorimetric	0.5−30	0.08	30
2	Papain-Ag NPs	colorimetric	0.25−50	0.079	37
3	smartphone-based CD-spectrometer	colorimetric	0.6250−40	0.4946	38
4	silica-coated Au nanorods	colorimetric	0.1−2.5	0.049	39
5	graphene quantum dots	colorimetric	0.3−10	0.094	40
6	CQDs	colorimetric	1.0−105	0.14	41
7	Cu−Ag/rGO	colorimetric	5−30	3.8	42
8	Mn-CDs	colorimetric	0.05−2.5	0.009	43
9	M-CQDs	colorimetric	10−70	3.26	44
10	IL-capped Ag NPs	colorimetric	0.002−3.22	0.013	this work

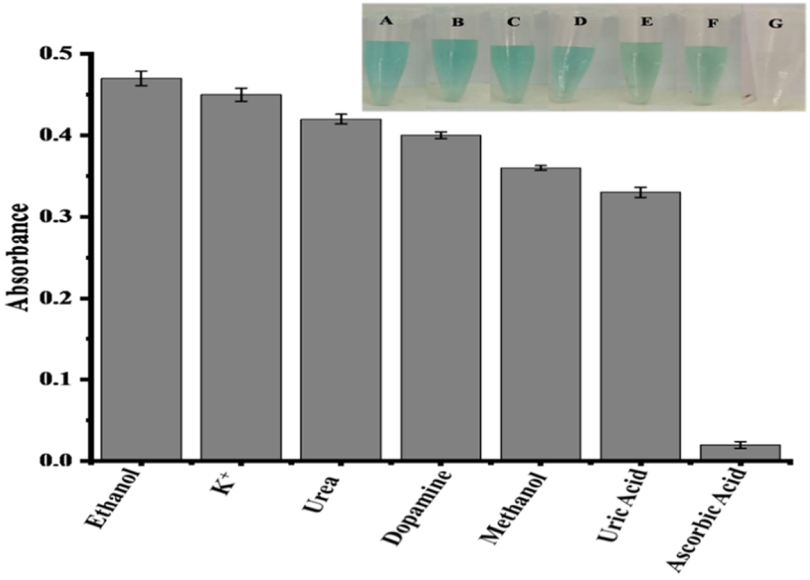

Figure 12. Interaction between ascorbic acid and other analytes at concentrations of (3.2×10^{-5} M).

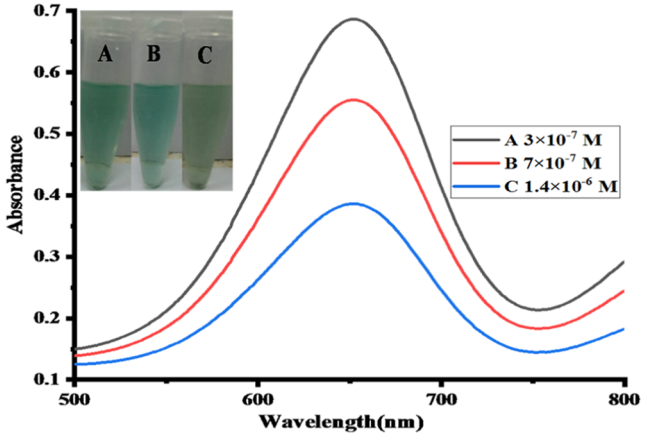

Figure 13. By the addition of different concentrations of ascorbic acid in the UV−vis spectra of the real samples of blood serum at optimized conditions (0.295×10^{-7}, 0.692×10^{-7}, and 1.37×10^{-6} M).

Table 3. Real-Sample Analysis of Blood Serum

sample	detected	ascorbic acid added (μM)	ascorbic acid found (μM)	recovery (%)	RSD (%)
1	0.005	0.295	0.3	101.69	0.838
2	0.008	0.682	0.7	101.15	1.009
3	0.03	1.37	1.4	102.18	0.459

3.4.5. Analytical Characteristics of the Proposed Biosensor. Under ideal experimental conditions, a simple colorimetric assay was used directly with the Ag NPs to detect various ascorbic acid concentrations. A sensitive and effective colorimetric method based on the relationship between the ascorbic acid concentration and absorbance intensity at 652 nm was used for the determination of ascorbic acid. The developed sensor's ascorbic acid detection sensitivity was evaluated by using a range of ascorbic acid concentrations. The response of colorimetric biosensors to varying ascorbic acid concentrations is shown in Figure 11A,B. At lower concentrations of ascorbic acid, the sensor response was low, and the peak absorbance was high, but as the ascorbic acid concentration increased, they linearly decreased. This method was able to detect ascorbic acid with a linear range of 2×10^{-9}−3.22×10^{-7} M and an R^2 value of 0.9996. It was found that both the LOQ and LOD were 1.30×10^{-8} and 4.3×10^{-8} M, respectively. The proposed colorimetric method had the advantages of a low limit of detection, direct eye observation, and low cost when compared to other previously reported detection methods. Table 2 compares this work with previously reported colorimetric methods on the basis of linear range and limit of detection for the colorimetric determination of ascorbic acid.

3.5. Interference Studies. In order to evaluate the selective detection of ascorbic acid employing IL-loaded Ag NPs, the absorbance sensitivity of the proposed biosensor was

https://doi.org/10.1021/acsomega.3c06353
ACS Omega 2023, 8, 44931−44941

examined with regularly coexisting samples such as ethanol, urea, methanol, K^+, dopamine, and uric acid, as shown in Figure 12. The results of Figure 12 show that ascorbic acid has a very low absorption value. Ethanol, urea, methanol, K^+, dopamine, and uric acid have substantially high absorption values. However, the absorbance spectra decrease only at 652 nm when the quantity of ascorbic acid is increased; there are noticeable changes in absorbance when coexisting compounds are added. The same experimental conditions and analyte concentration (3.22×10^{-5} M) were used for all of the experiments. As a result, the suggested sensor also showed great selectivity for the detection of ascorbic acid compared to concurrent interfering species. When compared to the existing literature, the reported approach for the detection of hydrogen peroxide has a higher selectivity. The impact of several interfering ions and chemicals, including glucose, dopamine, uric acid, and citric acid, as well as ions, was studied. Up to a concentration of 1 mM, it was found that the aforementioned ions and compounds had no discernible impact on the detection of ascorbic acid.

3.6. Real-Sample Analysis. The fabricated sensor is intended to verify the ascorbic acid measurement in a real specimen. In a blood serum sample from a scurvy patient, ascorbic acid is found under ideal experimental conditions. Ascorbic acid solutions with various concentrations, including 0.295×10^{-7}, 0.692×10^{-7}, and 1.37×10^{-6} M, were spiked into a blood serum sample solution from a scurvy patient that was received from a pharmacy, according to Figure 13. The calibration plot, which was previously created using multiple ascorbic acid concentrations collected under the same ideal conditions at 652 nm, is used to determine the actual ascorbic acid content in the serum total sample solution. The percentage recovery algorithm is used, and Table 3 provides a summary of the results

$$\text{recovery}\% = \text{ascorbic acid found}/\text{ascorbic acid added} \times 100$$

4. CONCLUSIONS

In this research, an ionic liquid-capped silver nanoparticle-based biosensor was fabricated for the detection of ascorbic acid. The silver nanoparticles were synthesized with the help of a paracetamol reductant, which is cost-effective, ubiquitously available, and easily handled. The proposed biosensor offers a sensitive and selective method for the determination of ascorbic acid with a linear range from 2×10^{-9} to 3.22×10^{-7} M, a low detection limit of 1.3×10^{-8} M, and a low quantification limit of 4.3×10^{-8} M. Comprehensive studies were carried out to achieve the best results for the proposed sensor. Different parameters, such as the TMB concentration, time, amount of capped NPs, and pH, were optimized. In addition, the proposed biosensor was successfully used for the detection of ascorbic acid in samples of human plasma. The proposed sensor has the potential to be used for commercial use.

AUTHOR INFORMATION

Corresponding Authors

Umar Nishan − *Department of Chemistry, Kohat University of Science and Technology, Kohat 26000 Khyber Pakhtunkhwa, Pakistan*; orcid.org/0000-0002-0106-3068; Email: umarnishan85@gmail.com

Suvash Chandra Ojha − *Department of Infectious Diseases, The Affiliated Hospital of Southwest Medical University, Luzhou 646000, China*; Email: suvash_ojha@swmu.edu.cn

Authors

Irfan Ullah − *Department of Chemistry, Kohat University of Science and Technology, Kohat 26000 Khyber Pakhtunkhwa, Pakistan*

Rukhsana Gul − *Department of Chemistry, Kohat University of Science and Technology, Kohat 26000 Khyber Pakhtunkhwa, Pakistan*

Amir Badshah − *Department of Chemistry, Kohat University of Science and Technology, Kohat 26000 Khyber Pakhtunkhwa, Pakistan*

Nawshad Muhammad − *Department of Dental Materials, Institute of Basic Medical Sciences Khyber Medical University, Peshawar 25100 Khyber Pakhtunkhwa, Pakistan*; orcid.org/0000-0001-6453-0658

Naeem Khan − *Department of Chemistry, Kohat University of Science and Technology, Kohat 26000 Khyber Pakhtunkhwa, Pakistan*

Mohibullah Shah − *Department of Biochemistry, Bahauddin Zakariya University, Multan 66000, Pakistan*; orcid.org/0000-0001-6126-7102

Muhammad Asad − *Department of Chemistry, Kohat University of Science and Technology, Kohat 26000 Khyber Pakhtunkhwa, Pakistan*

Saifullah Afridi − *Department of Chemistry, Kohat University of Science and Technology, Kohat 26000 Khyber Pakhtunkhwa, Pakistan*; orcid.org/0000-0003-2814-4738

Riaz Ullah − *Department of Pharmacognosy, College of Pharmacy, King Saud University, Riyadh 11451, Saudi Arabia*; orcid.org/0000-0002-2860-467X

Essam A. Ali − *Department of Pharmaceutical Chemistry, College of Pharmacy, King Saud University, Riyadh 11451, Saudi Arabia*

Complete contact information is available at: https://pubs.acs.org/10.1021/acsomega.3c06353

Funding

This research work was supported by the Doctoral Research Fund awarded to SCO. The authors thank researchers supporting Project number (RSP-2023R45) King Saud University, Riyadh, Saudi Arabia.

Notes

The authors declare no competing financial interest.

ACKNOWLEDGMENTS

The authors wish to thank the Researchers Supporting Project Number (RSP-2023R45) at the King Saud University Riyadh Saudi Arabia for financial support. The authors also thank the Doctoral Research Fund, China, for financial support.

REFERENCES

(1) Yin, R.; Mao, S.-Q.; Zhao, B.; Chong, Z.; Yang, Y.; Zhao, C.; Zhang, D.; Huang, H.; Gao, J.; Li, Z.; et al. Ascorbic acid enhances Tet-mediated 5-methylcytosine oxidation and promotes DNA demethylation in mammals. *J. Am. Chem. Soc.* **2013**, *135* (28), 10396−10403.

(2) Kim, J.-E.; Cho, H.-S.; Yang, H.-S.; Jung, D.-J.; Hong, S.-W.; Hung, C.-F.; Lee, W. J.; Kim, D. Depletion of ascorbic acid impairs

https://doi.org/10.1021/acsomega.3c06353
ACS Omega 2023, 8, 44931−44941

NK cell activity against ovarian cancer in a mouse model. *Immunobiology* **2012**, *217* (9), 873−881.
(3) Massey, L. K.; Liebman, M.; Kynast-Gales, S. A. Ascorbate increases human oxaluria and kidney stone risk. *J. Nutr.* **2005**, *135* (7), 1673−1677.
(4) Zhao, Y.; Li, Y.; Wang, Y.; Zheng, J.; Yang, R. A new strategy for fluorometric detection of ascorbic acid based on hydrolysis and redox reaction. *RSC Adv.* **2014**, *4* (66), 35112−35115.
(5) Bali Prasad, B.; Jauhari, D.; Tiwari, M. P. A dual-template imprinted polymer-modified carbon ceramic electrode for ultra trace simultaneous analysis of ascorbic acid and dopamine. *Biosens. Bioelectron.* **2013**, *50*, 19−27.
(6) Frenich, A. G.; Torres, M. H.; Vega, A. B.; Vidal, J. M.; Bolanos, P. P. Determination of ascorbic acid and carotenoids in food commodities by liquid chromatography with mass spectrometry detection. *J. Agric. Food Chem.* **2005**, *53* (19), 7371−7376.
(7) Dong, S.; Zhang, S.; Cheng, X.; He, P.; Wang, Q.; Fang, Y. Simultaneous determination of sugars and ascorbic acid by capillary zone electrophoresis with amperometric detection at a carbon paste electrode modified with polyethylene glycol and Cu_2O. *J. Chromatogr. A* **2007**, *1161* (1−2), 327−333.
(8) Rong, M.; Lin, L.; Song, X.; Wang, Y.; Zhong, Y.; Yan, J.; Feng, Y.; Zeng, X.; Chen, X. Fluorescence sensing of chromium (VI) and ascorbic acid using graphitic carbon nitride nanosheets as a fluorescent switch. *Biosens. Bioelectron.* **2015**, *68*, 210−217.
(9) Midha, K.; Singh, G.; Nagpal, M.; Arora, S. Potential application of silver nanoparticles in medicine. *Nanosci. Nanotechnol.* **2016**, *6* (2), 82−91.
(10) Li, K.; Wang, K.; Qin, W.; Deng, S.; Li, D.; Shi, J.; Huang, Q.; Fan, C. DNA-directed assembly of gold nanohalo for quantitative plasmonic imaging of single-particle catalysis. *J. Am. Chem. Soc.* **2015**, *137* (13), 4292−4295.
(11) Saha, K.; Agasti, S. S.; Kim, C.; Li, X.; Rotello, V. M. Gold nanoparticles in chemical and biological sensing. *Chem. Rev.* **2012**, *112* (5), 2739−2779.
(12) Wang, X.; Wu, P.; Hou, X.; Lv, Y. An ascorbic acid sensor based on protein-modified Au nanoclusters. *Analyst* **2013**, *138* (1), 229−233.
(13) Chen, Y. J.; Yan, X. P. Chemical redox modulation of the surface chemistry of CdTe quantum dots for probing ascorbic acid in biological fluids. *Small* **2009**, *5* (17), 2012−2018.
(14) Li, N.; Li, Y.; Han, Y.; Pan, W.; Zhang, T.; Tang, B. A highly selective and instantaneous nanoprobe for detection and imaging of ascorbic acid in living cells and in vivo. *Anal. Chem.* **2014**, *86* (8), 3924−3930.
(15) Zhai, W.; Wang, C.; Yu, P.; Wang, Y.; Mao, L. Single-layer MnO_2 nanosheets suppressed fluorescence of 7-hydroxycoumarin: mechanistic study and application for sensitive sensing of ascorbic acid in vivo. *Anal. Chem.* **2014**, *86* (24), 12206−12213.
(16) Frederix, F.; Friedt, J.-M.; Choi, K.-H.; Laureyn, W.; Campitelli, A.; Mondelaers, D.; Maes, G.; Borghs, G. Biosensing based on light absorption of nanoscaled gold and silver particles. *Anal. Chem.* **2003**, *75* (24), 6894−6900.
(17) Li, H.; Rothberg, L. Colorimetric detection of DNA sequences based on electrostatic interactions with unmodified gold nanoparticles. *Proc. Natl. Acad. Sci. U.S.A.* **2004**, *101* (39), 14036−14039.
(18) Liang, Y.; Ozawa, M.; Krueger, A. A general procedure to functionalize agglomerating nanoparticles demonstrated on nanodiamond. *ACS Nano* **2009**, *3* (8), 2288−2296.
(19) He, Z.; Alexandridis, P. Nanoparticles in ionic liquids: interactions and organization. *Phys. Chem. Chem. Phys.* **2015**, *17* (28), 18238−18261.
(20) Nishan, U.; Bashir, F.; Muhammad, N.; Khan, N.; Rahim, A.; Shah, M.; Nazir, R.; Sayed, M. Ionic liquid as a moderator for improved sensing properties of TiO_2 nanostructures for the detection of acetone biomarker in diabetes mellitus. *J. Mol. Liq.* **2019**, *294*, No. 111681.
(21) Nishan, U.; Niaz, A.; Muhammad, N.; Asad, M.; Shah, A. u. H.; Khan, N.; Khan, M.; Shujah, S.; Rahim, A. Non-enzymatic colorimetric biosensor for hydrogen peroxide using lignin-based silver nanoparticles tuned with ionic liquid as a peroxidase mimic. *Arabian J. Chem.* **2021**, *14* (6), No. 103164, DOI: 10.1016/j.arabjc.2021.103164.
(22) Nishan, U.; Sabba, U.; Rahim, A.; Asad, M.; Shah, M.; Iqbal, A.; Iqbal, J.; Muhammad, N. Ionic liquid tuned titanium dioxide nanostructures as an efficient colorimetric sensing platform for dopamine detection. *Mater. Chem. Phys.* **2021**, *262*, No. 124289.
(23) Nishan, U.; Ullah, W.; Muhammad, N.; Asad, M.; Afridi, S.; Khan, M.; Shah, M.; Khan, N.; Rahim, A. Development of a nonenzymatic colorimetric sensor for the detection of uric acid based on ionic liquid-mediated nickel nanostructures. *ACS Omega* **2022**, *7* (30), 26983−26991.
(24) Giri, A. K.; Jena, B.; Biswal, B.; Pradhan, A. K.; Arakha, M.; Acharya, S.; Acharya, L. Green synthesis and characterization of silver nanoparticles using Eugenia roxburghii DC. extract and activity against biofilm-producing bacteria. *Sci. Rep.* **2022**, *12* (1), No. 8383.
(25) Kaur, A.; Goyal, D.; Kumar, R. Surfactant mediated interaction of vancomycin with silver nanoparticles. *Appl. Surf. Sci.* **2018**, *449*, 23−30.
(26) Ashokkumar, R.; Ramaswamy, M. Phytochemical screening by FTIR spectroscopic analysis of leaf extracts of selected Indian medicinal plants. *Int. J. Curr. Microbiol. Appl. Sci.* **2014**, *3* (1), 395−406.
(27) Haider, A. J.; Jameel, Z. N.; Taha, S. Y. Synthesis and characterization of TiO_2 nanoparticles via sol-gel method by pulse laser ablation. *Eng. Technol. J.* **2015**, *33* (5), 761−771.
(28) Asad, M.; Muhammad, N.; Khan, N.; Shah, M.; Khan, M.; Khan, M.; Badshah, A.; Latif, Z.; Nishan, U. Colorimetric acetone sensor based on ionic liquid functionalized drug-mediated silver nanostructures. *J. Pharm. Biomed. Anal.* **2022**, *221*, No. 115043.
(29) Nishan, U.; Gul, R.; Muhammad, N.; Asad, M.; Rahim, A.; Shah, M.; Iqbal, J.; Uddin, J.; Ali Shah, A. u. H.; Shujah, S. Colorimetric based sensing of dopamine using ionic liquid functionalized drug mediated silver nanostructures. *Microchem. J.* **2020**, *159*, No. 105382, DOI: 10.1016/j.microc.2020.105382.
(30) Liu, X.; Wang, X.; Qi, C.; Han, Q.; Xiao, W.; Cai, S.; Wang, C.; Yang, R. Sensitive colorimetric detection of ascorbic acid using Pt/CeO_2 nanocomposites as peroxidase mimics. *Appl. Surf. Sci.* **2019**, *479*, 532−539.
(31) Chen, H.; Yuan, C.; Yang, X.; Cheng, X.; Elzatahry, A. A.; Alghamdi, A.; Su, J.; He, X.; Deng, Y. Hollow mesoporous carbon nanospheres loaded with Pt nanoparticles for colorimetric detection of ascorbic acid and glucose. *ACS Appl. Nano Mater.* **2020**, *3* (5), 4586−4598.
(32) Nishan, U.; Haq, S. U.; Rahim, A.; Asad, M.; Badshah, A.; Ali Shah, A.-u.-H.; Iqbal, A.; Muhammad, N. Ionic-liquid-stabilized TiO_2 nanostructures: a platform for detection of hydrogen peroxide. *ACS Omega* **2021**, *6* (48), 32754−32762.
(33) Nishan, U.; Khan, H. U.; Rahim, A.; Asad, M.; Qayum, M.; Khan, N.; Shah, M.; Muhammad, N. Non-enzymatic colorimetric sensing of nitrite in fortified meat using functionalized drug mediated manganese dioxide. *Mater. Chem. Phys.* **2022**, *278*, No. 125729.
(34) Nishan, U.; Ullah, I.; Muhammad, N.; Afridi, S.; Asad, M.; Haq, S. U.; Khan, M.; Soylak, M.; Rahim, A. Investigation of Silver-Doped Iron Oxide Nanostructures Functionalized with Ionic Liquid for Colorimetric Sensing of Hydrogen Peroxide. *Arabian J. Sci. Eng.* **2023**, *48*, 7703−7712, DOI: 10.1007/s13369-023-07791-z.
(35) Yang, X.-H.; Ling, J.; Peng, J.; Cao, Q.-E.; Wang, L.; Ding, Z.-T.; Xiong, J. Catalytic formation of silver nanoparticles by bovine serum albumin protected-silver nanoclusters and its application for colorimetric detection of ascorbic acid. *Spectrochim. Acta, Part A* **2013**, *106*, 224−230, DOI: 10.1016/j.saa.2012.12.097.
(36) Khaliq, A.; Nazir, R.; Khan, M.; Rahim, A.; Asad, M.; Shah, M.; Khan, M.; Ullah, R.; Ali, E. A.; Khan, A.; Nishan, U. Co-Doped CeO_2/Activated C Nanocomposite Functionalized with Ionic Liquid for Colorimetric Biosensing of H_2O_2 via Peroxidase Mimicking. *Molecules* **2023**, *28* (8), 3325.

https://doi.org/10.1021/acsomega.3c06353
ACS Omega 2023, 8, 44931−44941

(37) Peng, J.; Ling, J.; Zhang, X.-Q.; Zhang, L.-Y.; Cao, Q.-E.; Ding, Z.-T. A rapid, sensitive and selective colorimetric method for detection of ascorbic acid. *Sens. Actuators, B* **2015**, *221*, 708−716.
(38) Kong, L.; Gan, Y.; Liang, T.; Zhong, L.; Pan, Y.; Kirsanov, D.; Legin, A.; Wan, H.; Wang, P. A novel smartphone-based CD-spectrometer for high sensitive and cost-effective colorimetric detection of ascorbic acid. *Anal. Chim. Acta* **2020**, *1093*, 150−159.
(39) Wang, G.; Chen, Z.; Chen, L. Mesoporous silica-coated gold nanorods: towards sensitive colorimetric sensing of ascorbic acid via target-induced silver overcoating. *Nanoscale* **2011**, 3 (4), 1756−1759.
(40) Liu, J.-J.; Chen, Z.-T.; Tang, D.-S.; Wang, Y.-B.; Kang, L.-T.; Yao, J.-N. Graphene quantum dots-based fluorescent probe for turn-on sensing of ascorbic acid. *Sens. Actuators, B* **2015**, *212*, 214−219.
(41) Shu, X.; Chang, Y.; Wen, H.; Yao, X.; Wang, Y. Colorimetric determination of ascorbic acid based on carbon quantum dots as peroxidase mimetic enzyme. *RSC Adv.* **2020**, *10* (25), 14953−14957.
(42) Darabdhara, G.; Sharma, B.; Das, M. R.; Boukherroub, R.; Szunerits, S. Cu-Ag bimetallic nanoparticles on reduced graphene oxide nanosheets as peroxidase mimic for glucose and ascorbic acid detection. *Sens. Actuators, B* **2017**, *238*, 842−851.
(43) Zhuo, S.; Fang, J.; Li, M.; Wang, J.; Zhu, C.; Du, J. Manganese (II)-doped carbon dots as effective oxidase mimics for sensitive colorimetric determination of ascorbic acid. *Microchim. Acta* **2019**, *186* (12), No. 745, DOI: 10.1007/s00604-019-3887-6.
(44) Chandra, S.; Singh, V. K.; Yadav, P. K.; Bano, D.; Kumar, V.; Pandey, V. K.; Talat, M.; Hasan, S. H. Mustard seeds derived fluorescent carbon quantum dots and their peroxidase-like activity for colorimetric detection of H_2O_2 and ascorbic acid in a real sample. *Anal. Chim. Acta* **2019**, *1054*, 145−156.

https://doi.org/10.1021/acsomega.3c06353
ACS Omega 2023, 8, 44931−44941